Transaction of the Korean Society of Mechanical Engineers, Vol. 9, No. 1, pp. 119~126, 1985.

<Orginal>

Optimal Design of Structural Componets with Thickness and Shape Variatins†

Yung Myun Yoo*

(Received September 6, 1984)

두께와 모양 변화를 통한 구조물의 최적설계

유 영 면

Key Word: Optimization, Structural, Thickness, Shape, Variations

초 록

형상은 3차원이지만 2차원 문제로 이상화하여 해석할 수 있는 탄성구조물의 최적설계를 내연기관 연결봉(Connecting Rod)을 예제로 사용하여 진행하였다. 연결봉은 각 부위에서의 두께는 다르나 평면응력상태에 있다고 가정하였다. 연결봉의 질량을 최소화하기 위해 두께의 분포 및 2차원 모델 경계의 모양을 설계변수로 채택하였고 설계변수 및 응력치에 대한 제한조건을 적용하였다. 설계감도 계수 계산을 위해 Variational Formulation, Material Derivative, Adjoint Variable 이론을 도입하였고 최적화 방법으로는 Gradient Projection Method를 사용하였다. 최적설계 결과 현재 사용중인 연결봉 무게의 20%를 줄일 수 있음이 밝혀졌다.

1. Introduction

An extenive literature has developed on optimization of structures and structural components whose shapes are defined by cross section and thickness variables[1]. In most treatments of such structural design problems, calculus of variations on a fixed domain and an adjoint variable technique are used to calculate design sensitivity. Shape optimization for problems of applied physics has been investigated extensively by Cea, using variational methods of boundary-value problem formulation[2]. In this paper a variational formulation of the equations of elasticity, the material derivative of continuum mechanics, and an adjoint variable technique are pressented for calculation of design sensitivity of a functional defined on a domain whose shape is continuously changed. The procedure developed has been successfully applied for shape optimization of simple elastic structures in references 3 and 4. The theories are combined here for optimization of an engine connecting rod whose thickness distribution and shape are taken as design variables.

†Presented at the KSME Spring Conference, 1984

*Member, CAD/CAM Research Laboratory, The Korea Advanced Institute of Science and Technology

2. Description of the Structural Component

An engine connecting rod connects the crank shaft and piston pin of an engine, transmitting axial compressive load during firing and axial tensile load during the suction cycle of the exhaust stroke. The gemetry of the connecting rod considered is shown in Fig. 1. Considering that the loads acting on the rod are in a plane and the rod deforms mainly in a plane, one can reasonably assume that the rod is in a plane stress state.

The domain and boundary of the system are denoted as Ω and Γ, respectively. The boundary Γ is composed of six parts; Γ_1 through Γ_6, as shown in Fig. 2. Segments Γ_1 and Γ_2 are boundaries at which the connecting rod touches the crank shaft and the piston pin, respectively, Their shapes are fixed during the design process. The boundaries Γ_3 and Γ_5 of the shank and neck regions of the rod are to be determined through the optimization process. Since the main interest of shape opt-

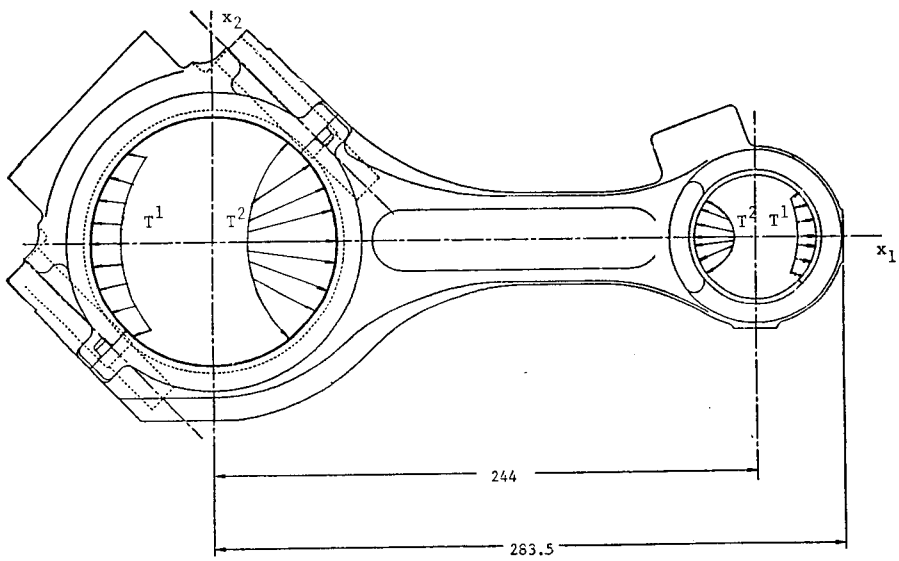

Fig. 1 Engine connecting rod

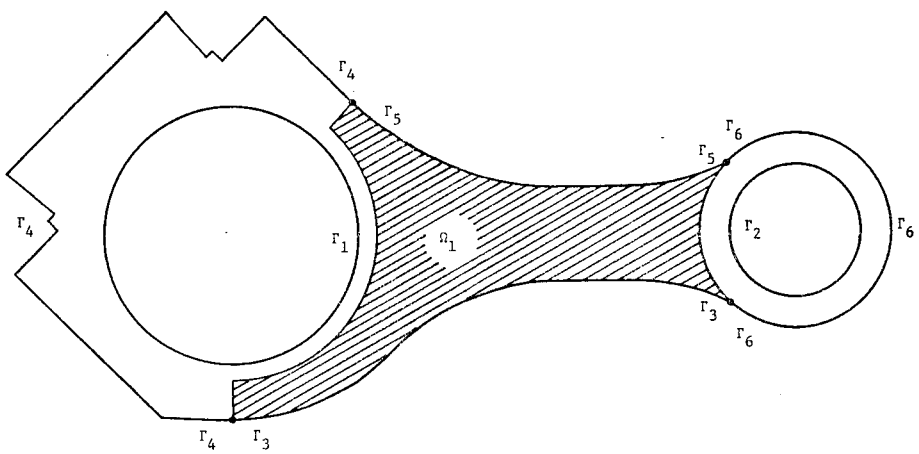

Fig. 2 Boundaries and Ω_1

imal design rests on the shank and neck regions, one may keep the shape of boundaries Γ_4 and Γ_6 fixed. In shape optimization of the connecting rod, one wishes to determine the optimum thickness distribution, which varies independently from the domain shape variation, as well as the shapes of Γ_3 and Γ_5. With the main interest on the shank and neck regions, thickness distribution in the hatched area Ω_1 of Fig. 2 is to be determined through the optimization process.

To satisfy the condition that the distance between the piston pin and the crank shaft is prescribed, it is required that every point in the rod not move in the x_1-direction. Hence, points on Γ_3 and Γ_5 are allowed to move only in the x_2-direction.

Since the system is assumed to be quasi-static, without body force, boundary conditions are

$$\left.\begin{aligned} &T_m{}^l=\sigma^{mn}(z^l)n_m,\ m=1,2,\ l=1,2,\ \text{on } \Gamma \\ &z^l=[z_1{}^l, z_2{}^l]^T=0,\ l=1,2,\ \text{at one point } A \\ &z_2{}^l=0,\ l=1,2,\ \text{at another point } B \end{aligned}\right\} \quad (1)$$

where T^l, z^l, and n are two dimensional vectors of surface traction, displacement due to T^l, and outward unit normal on Γ, resectively. The superscript l denotes the loading case ($l=1$ for inertia load and $l=2$ for firing load, as shown in Fig. 1 and $\sigma^{ik}(z^l)$ denotes components of the stress tensor due to displacement z^l. The kinematic boundary conditions of Eq. 1 are imposed to eliminate rigid body motion of the rod, which is reasonable because the loads acting on the rod are in self-equilibrium. For convenience, point A is selected on Γ_4 and point B is on Γ_6, where shapes are not changed.

One can define a set Z of kinematically admissible displacements of the system as

$$z=\{z=[z_1, z_2]^T : z\in[H^1(\Omega)]^2,\ z=0 \text{ at point } A \text{ and } z_2=0 \text{ at point } B\} \quad (2)$$

where $[H^1(\Omega)]^2\equiv H^1(\Omega)\times H^1(\Omega)$ is the product of Sobolev spaces of order one[5]. The variational form of the equations of elasticity for the system is to find $z^l\in Z$ that satify

$$\int_\Omega \sigma^{mn}(z^l)\varepsilon^{mn}(\bar{z})hd\Omega=\int_\Gamma hT^l\cdot\bar{z}d\Gamma,\ l=1,2 \quad (3)$$

for all virtual displacements $\bar{z}\in Z$, where h and $\varepsilon^{mn}(\bar{z})$ denote the thickness distribution function in Ω and components of the strain tensor when one treats $\bar{z}$ as a displacement vector, respectively. One can use the finite element method to solve Eq. 3 numerically.

3. Formulation of the Optimal Design Problem

Volume of the connecting rod is the cost functional in the design process,

$$\Psi_0=\int_\Omega hd\Omega \quad (4)$$

The design problem is to find the shapes of Γ_3 and Γ_5 and the thickness distribution h in Ω_1, subject to the following conditions:

3.1. Stress Constraints

Lower and upper bounds are imposed on principal stresses of inertia and firing loads, in the form

$$\left.\begin{aligned} &\sigma_1{}^1<\sigma_{UI},\ \text{in } \Omega \\ &\sigma_{LI}<\sigma_2{}^1,\ \text{in } \Omega \end{aligned}\right\} \quad (5)$$

for the inertia load and

$$\left.\begin{aligned} &\sigma_1{}^2<\sigma_{UF},\ \text{in } \Omega \\ &\sigma_{LF}<\sigma_2{}^2,\ \text{in } \Omega \end{aligned}\right\} \quad (6)$$

for the firing load, where σ_{LI} and σ_{UI} denote lower and upper bounds on principal stress of the inertia load and σ_{LF} and σ_{UF} correspond to those of the firing load. In Eqs. 5 and 6, $\sigma_1{}^l$ and $\sigma_2{}^l$ denote principal stresses of loading case l,

$$\sigma_1{}^l=\frac{\sigma^{11}(z^l)+\sigma^{22}(z^l)}{2}+\sqrt{\left[\frac{\sigma^{11}(z^l)-\sigma^{22}(z^l)}{2}\right]^2+(\sigma^{12}(z^l))^2} \quad (7)$$

$$\sigma_2{}^l=\frac{\sigma^{11}(z^l)+\sigma^{22}(z^l)}{2}-\sqrt{\left[\frac{\sigma^{11}(z^l)-\sigma^{22}(z^l)}{2}\right]^2+(\sigma^{12}(z^l))^2}$$

3.2. Thickness Constraint

Thickness h in the hatched area of Fig. 2 must be bounded away form zero. Hence, the thickness constraint is given as

$$-h+c\leq 0, \text{ in } \Omega \tag{8}$$

where h and $c>0$ denote the thickness distribution function and its lower bound, respectively.

The pointwise constraints of Eqs. 5 and 6 ear transformed to functional constraints on every finite element, using a mollifier or averaging method[4], as

$$\psi^l{}_{ij}=\int_{\Omega_j} M_j\phi_i{}^l d\Omega=\int_{\Omega} M_j\phi_i{}^l d\Omega\leq 0,$$
$$j=1,\cdots\cdots,\text{NEL},\ i=1,2,\ l=1,2 \tag{9}$$

where NEL, Ω_j, and M_j denote the number of elements, the subdomain of each element, and a mollifier function($M_j>0$, $M_j=0$ off Ω_j, and $\int_{\Omega_j} M_j d\Omega=1$) defined on Ω_j. In Eq. 9, the indices l and i denote loading and principal stress numbers, respectively, and $\phi_i{}^l$ is a function of principal stresses, which is obtained from Eqs. 5 and 6; e.g.,

$$\phi_2{}'=-\sigma_2{}'+\text{constant} \tag{10}$$

in eq. 5.

4. Design Sensitivity Analysis

Before speaking of an optimum shape, one must define variation of the shape of a component. The approach adopted here is illustrated in Fig. 3, using the idea of a design velocity field $V(X)$ that defines the direction of movement of all points X in the nominal domain Ω to points x in a deformed domain Ω_t, given by the transformation $x=X+tV(X)$. As the step size parameter t approaches 0, the deformed domain Ω_t approaches the undeformed domain; i.e., $\Omega=\Omega_0$.

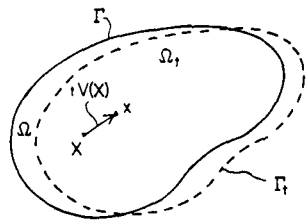

Fig. 3 Domain shape variation

For a given design velocity V, one may write the state z^l as a function of t; i.e., $z_t{}^l(X+tV(X))$. Defining $z^{l\prime}=\partial z_t{}^l(X)/\partial t$, one may use the material derivative of continuum mechanics[3,4] to calculate the variation of an integral $\Psi=\int_{\Omega_t} G(z_t{}^l)d\Omega_t$, to obtain

$$\delta\Psi=\int_{\Omega} G_{z^l}z^{l\prime}\ d\Omega+\int_{\Gamma} G(z^l)V\cdot n\ d\Gamma \tag{11}$$

where n is the outward unit normal on the boundary Γ. The first term in Eq. 11 may be viewed as taking the derivative with respect to t inside the integral and the second term represents the contribution due to normal movement $V\cdot n$ of the boundary. Using Eq. 11, one obtains

$$\delta\Psi_0=\int_{\Omega}\delta h d\Omega+\int_{\Gamma} hV\cdot n d\Gamma \tag{12}$$

$$\delta\Psi_{ij}{}^l=\int_{\Omega} M_j\frac{\partial\phi_i{}^l}{\partial\sigma^{mn}}\sigma^{mn}(z^{l\prime})d\Omega \tag{13}$$

while Eq. 12 is written directly in terms of design variations, Eq. 13 involves the directional derivative $z^{l\prime}$ of state. To rewrite this term as a function of design variation, one interprets the first term on the right of Eq. 13 as a virtual work that is associated with a virtual displacement $z^{l\prime}$ and defines λ^{ijl} as the solution of the adjoint equation

$$\int_{\Omega}\sigma^{mn}(\lambda^{ijl})\varepsilon^{mn}(\bar{\lambda})h d\Omega=\int_{\Omega} M_j\frac{\partial\phi_i{}^l}{\partial\sigma^{mn}}\sigma^{mn}(\bar{\lambda})d\Omega \tag{14}$$

which must hold for all $\bar{\lambda}\in Z$. One may now take the variation of both sides of Eq. 3 to obtain

$$\int_\Omega \{\sigma^{mn}(z^{l'})\varepsilon^{mn}(\bar{z})h+\sigma^{mn}(z^{l})\varepsilon^{mn}(\bar{z}')h +\sigma^{mn}(z^{l})\varepsilon^{mn}(\bar{z})\delta h\}d\Omega +\int_\Gamma \sigma^{mn}(z^{l})\varepsilon^{mn}(\bar{z})hV\cdot n d\Gamma =\int_\Gamma hT^{l}\cdot\bar{z}'d\Gamma \tag{15}$$

which must hold for all $\bar{z}\in Z$. In this example, $\bar{z}'$ is kinematically admissable, so since z^l is the solution of Eq. 3, terms involving $\bar{z}'$ in Eq. 15 cancel.

To evaluate the term on the right of Eq. 13, one may now evaluate Eq. 14 at $\bar{\lambda}=z^{l'}$, Eq. 15 at $\bar{z}=\lambda^{ijl}$, use Betti's reciprocal formula, and obtain

$$\delta\Psi_{ij}{}^{l}=-\int_\Omega \sigma^{mn}(z^{l})\varepsilon^{mn}(\lambda^{ijl})\delta h d\Omega -\int_\Gamma \sigma^{mn}(z^{l})\varepsilon^{mn}(\lambda^{ijl})h\,V\cdot n\,d\Gamma \tag{16}$$

To use this result comptationally, one may parameterize the thickness function $h(x_1, x_2)$ to be piecewise constant over strips of finite elements running along the shank. In the present model, 48 such strips are defined, as shown in Fig. 4. Similarly, one may parameterize the boundary by making it piecewise linear, defining the distance of nodes at corner points from the centerline of the rod as design parameters. In this example, 38 such boundary node locations are taken as design parameters, as shown in Fig. 5, for a total of 86 design parameters. One may thus write expressions for thickness variation in terms of design parmeter variation, in the form $\delta h=B(x_1, x_2)\delta b$ in and normal movement of the boundary as $V\cdot n=A(x_1, x_2)\delta b$ on Γ. Substituting these expressions into Eqs. 12 and 16, one has

$$\delta\Psi_0=\left[\int_\Omega B(x_1, x_2)d\Omega +\int_\Gamma h(x_1, x_2)A(x_1, x_2)d\Gamma\right]\delta b \tag{17}$$

$$\delta\Psi_{ij}{}^{l}=-\left[\int_\Omega \sigma^{mn}(z^{l})\varepsilon^{mn}(\lambda^{ijl})B(x_1, x_2)d\Omega +\int_\Gamma \sigma^{mn}(z^{l})\varepsilon^{mn}(\lambda^{ijl})hA(x_1, x_2)d\Gamma\right]\delta b \tag{18}$$

5. Optimization Algorithm

With the preceding design sensitivity analysis results, one can apply an iterative optimization algorithm. In this paper, a gradient projection methed[6] is used to numberically solve the optimal design problem; i.e., find a design that minimizes the cost functional Ψ_0, subject to the constraints

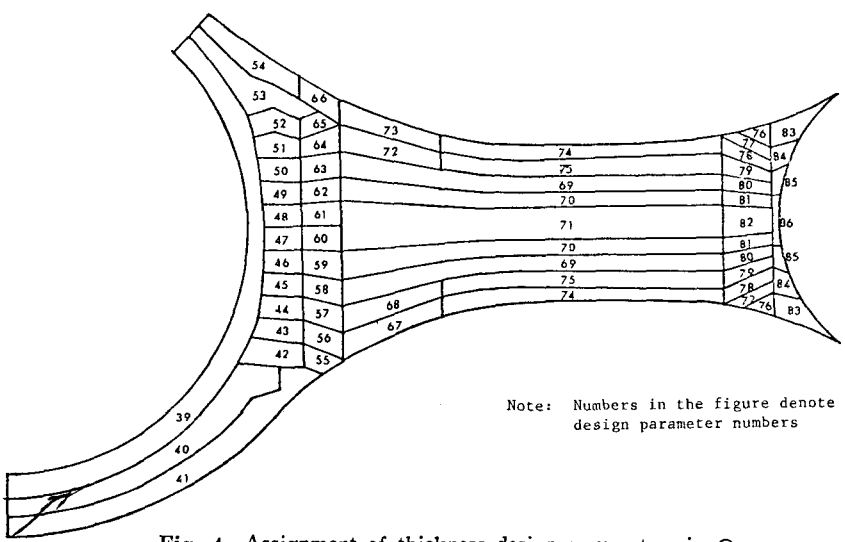

Fig. 4 Assignment of thickness design parameters in Ω_1

$$\left.\begin{aligned}&\Psi_p=0,\ p=1,2,,q'\\&\Psi_p\leq 0,\ p=q'+1,,q\end{aligned}\right\} \tag{19}$$

Equations 17 and 18 can be written, in general form, as

$$\delta\Psi_p=l^{pT}\delta b,\ p=0,1,\cdots,q \tag{20}$$

where l^p denotes the design sensitivity vetor. If $\Delta\Psi_p$ is the desired change in constraint p, one wishes to find δb to decrease Ψ_0 as possible and to satisfy

$$l^{pT}\delta b\begin{cases}=-\Delta\Psi_p,\ p=1,\cdots,q'\\\leq-\Delta\Psi_p,\ \Psi_p\geq-\varepsilon,\ p=q'+1,\cdots,q\end{cases} \tag{21}$$

where ε is a small positive constant defining those inequality constraints that are treated as ε-active.

In order to assure that the linear approxmations employed in obtaining Eqs. 20 and 21 are valid, it is demanded that δb be small in the quaratic sense; i.e.,

$$\delta b^T W\delta b=\xi^2 \tag{22}$$

where ξ is a small parameter and W is a positive definite weighting matrix. For convenience, deifne a set of indices

$$A=\{\alpha:\alpha=1,\cdots,q',\ \text{and}\ \alpha>q'\ \text{for which}\ \Psi_\alpha(z^0,b^0)\geq-\varepsilon\}$$

and a column vector $\tilde{\Psi}$ of elements Ψ_α with $\alpha\in A$,

$$\Psi=\left[\begin{matrix}\Psi_\alpha\\ \sigma\in A\end{matrix}\right] \tag{23}$$

The generalized steepest descent algorithm[6] used here is summarized as follows:

Step 1. Make an engineering estimate b^0 of the optimum design.

Step 2. Solve Eq. 3 for z^0, corresponding to b^0.

Step 3. Check constraints and form $\tilde{\Psi}$ of Eq. 23.

Step 4. Solve adjoint equations given by Eq. 14 for constraints $\tilde{\Psi}$.

Step 5. Compute l^p in Eq. 20 and form $\tilde{l}$ corresponcing to the costraints in $\tilde{\Psi}$.

Step 6. Choose $\Delta\tilde{\Psi}$ and the step-size parameter γ_0 on the first iteration. Hold γ_0 constant or adjust to speed convergence.

Step 7. Compute $M_{\Psi\Psi}$ and $M_{\Psi\Psi_0}$, given as

$$M_{\Psi\Psi_0}=\tilde{l}^T W^{-1}l^0 \tag{24}$$

$$M_{\Psi\Psi}=\tilde{l}^T W^{-1}\tilde{l} \tag{25}$$

Steep 8. Calculate $\tilde{\mu}$, $\tilde{\mu}^1$, and $\tilde{\mu}^2$ from

$$M_{\Psi\Psi}\tilde{\mu}^1=-M_{\Psi\Psi_0} \tag{26}$$

$$M_{\Psi\Psi}\tilde{\mu}^2=\Delta\Psi \tag{27}$$

$$\tilde{\mu}=\tilde{\mu}^1+2\gamma_0\tilde{\mu}^2 \tag{28}$$

If any component of $\tilde{\mu}$ is negative, delete the corresponding component of $\tilde{\Psi}$ and return to Step 3, otherwise contiune.

Step 9. Compute δb^1 and δb^2 given by

$$\delta b^1=W^{-1}[l^0+\tilde{l}\tilde{\mu}^1] \tag{29}$$

$$\delta b^2=W^{-1}\tilde{l}\tilde{\mu}^2 \tag{30}$$

Step 10. compute

$$b=b^0+\left(-\frac{1}{2\gamma_0}\delta b^1+\delta b^2\right) \tag{31}$$

Step 11. If $|\Psi_0(b)-\Psi_0(b^0)|$ and $\|\delta b^1\|$ are sufficiently small, terminate. Otherwise return to Step 2 with b^0 replaced by b.

6. Numerical Results

Numerical results presented in this paper are based on the following input data: $E=2.07\times10^5$MPa, $\nu=0.298$, $\sigma_{UI}=136$MPa, $\sigma_{LI}=-80$ MPa, $\sigma_{UF}=36$MPa, and $\sigma_{LF}=-279$MPa. The load vector for finite element analysis was generated from boundary force data supplied by the manufacturer of the connecting rod.

Regridding, to account for shape modification is carried out as follows:

(i) x_2-coordinates of nodal points on the varied boundaries at which design parameters are assigned are determined by the new design parameter vector.

(ii) x_2-coordinates of other nodal points on the varied boundaries are obtained by

linear interpolation between the nodal points that are determined by the new design parameter vector.

(iii) Coordinates of nodalpoints inside the domain are not changed, to match the assumption that h is varied independently from the domain variation.

In each design iteration, Eq. 9 is checked for every element. Those constraints that are not ε-active ($\varepsilon=0.02$) are discarded, so that one can save computation time. Hence, the number of constraints is changed in each design iteration.

Triangular elements with linear shape functions are used in the finite element analysis, as show in Fig. 5, with1014 grid points (2025 degrees of freedom) and 1717 elements. With the initial shape and thickness distribution,

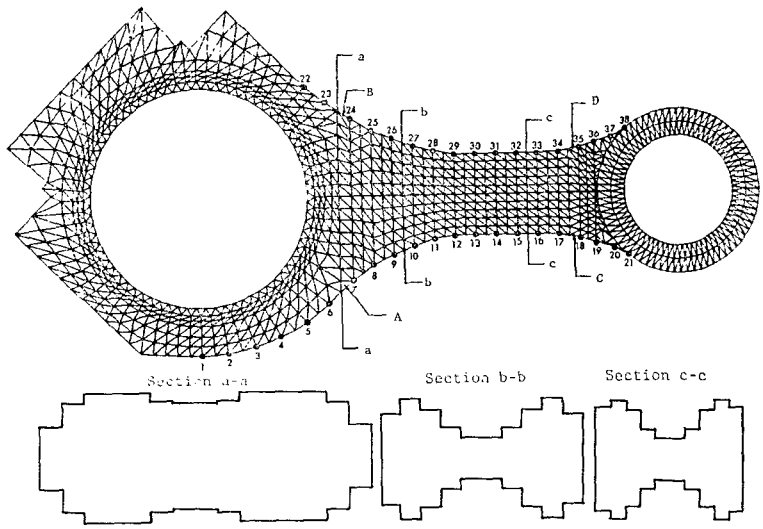

Fig. 5 Finite element model of engine connecting rod

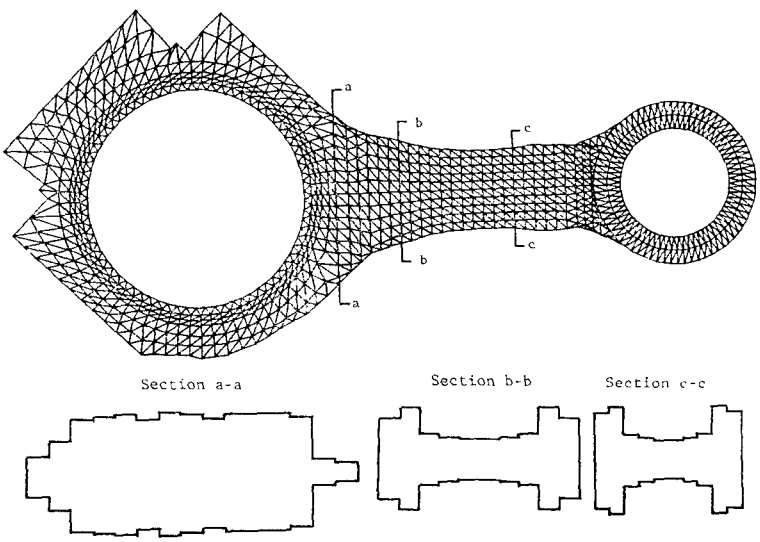

Fig. 6 Optimum design

upper bound constraints on the first principal stress of the firing loading are active in several elements in the neck area (near cross section a-a) in Fig. 5. The cost functional and $\|\delta b^1\|$ were initally $7.05\times10^5 mm^3$ and 1.97×10^3, respectively. After 98 design iterations, they are reduced to $6.42\times10^5 mm^3$ and 9.72×10^2, respectively, with 29 stress constraints active. Computer time on a PRIME 750 supermini computer was 4.2cpu minutes per iteration and a practical, near opimum design shown in Fig. 6 was obtained in 15 iterations.

7. Conclusions

A variational formulation of the governing equations, the material derivative idea, and an adjoint variable technique are combined for design sensitivity analysis of a functional defined on a domain whose shape is continuously changed. In view of theory and results presented, it is felt that there would be no fundamental conceptual or computational difficulties in applying the procedure to other optimal design problems of $2\frac{1}{2}$dimensional elastic structures.

Numerical experimentation with the procedure shows that the choice of numerical methods for calculation, especially the finite element method, is crucial in the procedure's success. This is mainly due to the fact that one obtains relatively poor stress results near the boundary, which is extensively used for sensitivity calculation. Therefore, an extensive research effort is desirable in this area. Also, application of mollifier function, defined on the domain of each element, for stress constrains needs more study because stress concentration always occurs on the boundaries of structures.

Reference

(1) Haug, E.J., "A Review of Distributed Parameter Structural Optimization Literature", *Optimization of Distributed Parameter Structures*, (Ed. E.J. Haug and J. Cea), Sijthoff & Nooıdhoff, Alphen aan den Rijn, Netherlands, pp. 3~74, 1981

(2) Cea, J., "Problems of Shape Optimal Design", *Optimization of Distributed Parameter Structures*(ed. E.J. Haug and J. Cea), Sijthoff & Noordhoff, Alphen aan den Rijn, The Netherlands, pp. 1005~1048, 1981

(3) Haug, E.J., Choi, K.K., Hou, J.W., and Yoo, Y.M., "A Variational Method for Shape Optimal Design of Elastic Structures", *Optimum Structural Design* Ⅱ (ed. R.H. Gallagher), Wiley, New York, 1983

(4) Haug, E.J., Choi, K.K., and Komkov, V., *Desing Sensitivity Analysis of Structural Systems*, Academic Press, New York, 1983

(5) Aubin, J-P., *Applied Functional Analysis*, Wiley-Interscience, New York, 1979

(6) Haug, E.J., and Arora, J.S., *Applied Optimal Design*, Wiley-Interscience, New York, 1979